

REMOTE SENSING WITH TDMF RADAR: SOME PRELIMINARY RESULTS

S. H. Yan

The State Key Laboratory of Information Engineering in Surveying,
Mapping and Remote Sensing
School of Electronic Information
Wuhan University
Wuhan, Hubei 430079, China

X. B. Wu and Z. Z. Chen

School of Electronic Information
Wuhan University
Wuhan, Hubei 430079, China

Abstract—HF radar in ocean remote sensing makes use of electromagnetic waves of 10 m to 100 m wavelength from the rough sea surface to measure surface current and ocean wave parameter. Recently, a new time division multiple frequency HF radar system called OSMAR2009 has been developed by the Wuhan University. One main advantage of the system is that it is of great help in extracting current parameters and significant wave height. A further advantage is the ability to avoid interference. In addition, this technique offers the opportunity to measure the current shear. These advantages are gained by transmitting time division multiple frequency chirp instead of one frequency chirp. This paper introduces the technical design and the advantage of OSMAR2009 and describes the remote sensing experiment implemented in East China Sea during 2009, followed by the field results and the brief analysis of such results.

1. INTRODUCTION

During the last decades multiple radar systems operating in different frequency bands have become useful tools for oceanographic research and target detection due to their remote sensing capability based on the Electromagnetic Scattering Theory [1–3]. HF radar takes the vertically

Corresponding author: S. H. Yan (ysh567@sohu.com).

polarized electromagnetic wave that “adheres” to the ocean surface and follows the air-water interface around the curvature of the Earth. Therefore, this radar can detect information over large coastal ocean areas. Some HF radar systems have been developed, such as seasonde from Codar Ocean Sensors Ltd, WERA in Germany (University of Hamburg) and multifrequency coastal radars (MCR’s) developed by the University of Michigan. In China, Wuhan University has been doing research on HF radar to extract sea state parameters for about twenty years, and several radar systems, such as OSMAR2000 [4] and OSMAR2003, have been used in Shanghai, China for sea environment monitoring.

Though HF radar systems are now commercially available, some problems still exist in the research on HF radar system. For example, operators are puzzled at how to choose the operating frequency, and ocean scientists still have doubts about the result of wave inverted by HF radar.

Wuhan University has developed a new time division multiple frequency (TDMF) radar system which can help further research on inversion of ocean state parameters. A field experiment was carried out to explore the capabilities of this system for monitoring along the East China Sea coast. This paper introduces the radar and field experimental results.

2. ADVANTAGES OF TDMF RADAR

Multiple frequency radar is very helpful in wave inversion. The hydrodynamic and electromagnetic analysis, both of which use perturbation expansions to describe the ocean surface and scattered electromagnetic field, are the base of wave inversion. According to perturbation theory, the low operating frequency systems do not have problems with radar spectral saturation or the spreading of the first-order line over the neighboring second-order structure. Low frequency systems also have far detection range since operating frequency is the dominating factor influencing the propagation loss of the electromagnetic wave in surface wave mode. The disadvantage of low frequency systems is that the second-order structure often falls below the noise floor, inhibiting the extraction of wave information.

When increasing the radar operating frequency, the second-order radar spectrum increases while the noise does not, which is helpful for extracting wave information. But the disadvantages of high operating frequency are as follows: first, the frequency width of the first-order spectrum increases and may cover the second-order spectrum when the current speed is high. Second, the saturation limit on wave

height decreases, meaning that information about the high waves, which researchers are often interested in, is not provided. Therefore, researchers face a frequency selection dilemma.

TDMF radar operates both in low and high frequencies in a coherent integration time (CIT), which gives the researchers the opportunity to study the Doppler spectrum of the backscatter signals at different sea states. It can also detect far target by low operating frequency and extract wave information by high operating frequency. In addition, TDMF radar is an important way to avoid interference, since the performance of the HF radar is seriously limited by the crowded interference from environment.

As shown by Teague et al. [5], HF radars operating at different frequencies measure near surface currents at different 'effective' depths. That is to say, multiple frequency enables the TDMF radar to map the current shears. It also offers an opportunity to perform HF radar target "RCS Spectroscopy", which holds promise for the classification of targets.

TDMF radar with time dividing multiple frequencies, instead of an absolutely simultaneous multiple frequencies, can reduce unnecessary complexity of radar receiver, transmit system and prevent combined interference of different frequencies. Considering the relatively slow change of sea state and low velocity ships, a proper CIT (for target about 3 minutes, for sea state about 10 minutes) is designed. Therefore, TDMF radar is suitable for measuring sea state and detecting target.

3. EXPERIMENT SETUP

3.1. OSMAR2009 Radar System

The OSMAR2009 system uses a time division frequency modulated interrupted continuous wave (FMICW) waveform. Fig. 1(a) depicts the frequency division of the waveform with two operating frequency bands. At every operating frequency band, the signal frequency chirp up in a time and chirp back down quickly. Fig. 1(b) shows basic layout of the TDMF radar system, including the antenna array, receiver, transmitter, sampling computer and processing computer. The radar parameter is completely configured and controlled from a graphical user interface (GUI) operating under the Windows 2000 operating system. Fig. 2 shows some components of OSMAR2009 system located in Zhujiajian Island.

The FMICW signal was generated by a frequency synthesizer with two DDS (digital direct synthesizer) chips driven by the same 200 MHz

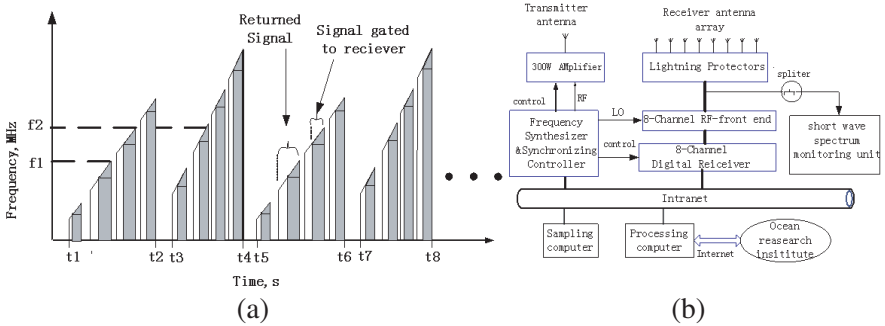


Figure 1. (a) The TDMF waveform with two operating frequency bands. (b) Basic layout of the TDMF HF radar system.

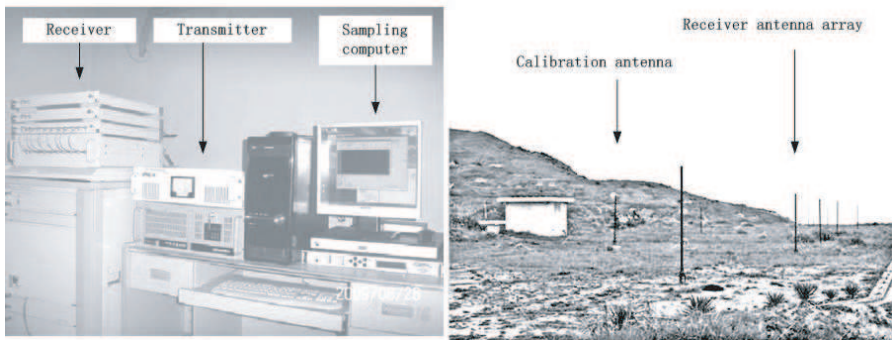


Figure 2. Receiver, transmitter, sampling computer and receiver antenna array of the radar system located in Zhujiajian Island.

TCXO (Temperature compensate crystal oscillator), after which the signal was sent to the transmitter and antennas.

The receiver consists of low noise amplifiers, radio frequency (RF) pre-selection filters, down converting mixers, and intermediate frequency (IF) amplifiers along with IF filter. The local oscillator (LO) signal for driving the mixer is derived from a DDS and amplified by a LO amplifier. After mixing, the IF is 41.4 MHz. The LO power is set at 27 dBm, through which the receiver can get a large dynamic range. The analog IF signal is band-pass sampled by the analog-to-digital converter (ADC) at IF and demodulated in programmable digital down-converters. Such a receiver structure offers more flexibility and less sensitivity to analog components than the traditional receiver employing analog IF processing. The output baseband complex signals are transported to PC through the LXI interface.

The transmit antenna is composed of three wide band monopole antennas and its impedance matching is provided by OSMAR2009 Internal broad preamplifiers and filters over the 3–30 MHz. Since phased array technology uses multiple antenna cells and electronic time delays to create beams that can be scanned and focused electronically for multiple angle inspections [6], the receive antenna array of OSMAR2009 is based on eight wide band helical antenna cells with 2 rows, and the first of which is a linear array combined by six cells for array signal processing while the second is combined by the other two antenna cells for array calibrating.

3.2. Experiment Setup

The East China Sea experiment was designed to validate the performance of TDMF radar, including the accurate sea current and wave height measurements. The radar worked with three frequencies: 8.56 MHz, 12.5 MHz and 16.8 MHz. The transmit power was 150 W. Two radar systems were installed at different sites as shown in Fig. 3. One site was located on Zhujiajian Island ($29^{\circ}53'24''\text{N}$, $122^{\circ}24'46''\text{E}$), while the other was located on Shengshan Island ($30^{\circ}42'16''\text{N}$, $122^{\circ}49'54''\text{E}$), both of which had a direct view of study area on the sea surface. Radial maps for both sites were produced in every 10 minutes. Two maps of radial current components were combined to obtain the vector velocity field. Some conventional instruments, including the

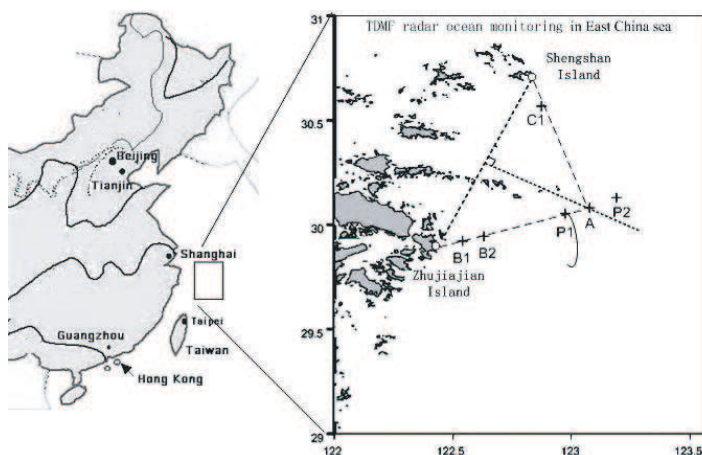


Figure 3. Radar site diagram showing two radar locations and measure points.

Acoustic Doppler Current Profiler (ADCP), Aanderaa Doppler current sensor (DCS), Directional buoy and Waverider buoys, were used to record the real-time sea state information at the six locations A, B1, B2, C1, and P1, P2.

In this paper, the radar estimated results are compared with those data from ADCP and drifter. The differences between two datasets are computed, and their statistics are quantified as follows:

mean absolute error (MAE) $m_{\Delta} = \frac{1}{n} \sum_{i=1}^N (x_i - y_i)$, root-mean-square (RMS) error: $\sigma = \sqrt{\frac{1}{n} \sum (x_i - y_i)^2}$ correlation coefficient (R): $R = \frac{\sum X_i Y_i - n \bar{X} \bar{Y}}{\sqrt{[\sum X_i^2 - n \bar{X}^2][\sum Y_i^2 - n \bar{Y}^2]}}$ where x_i are the parameters estimated by radar, and y_i are recorded by instrument respectively. n is the sample number.

4. RESULTS AND CONCLUSION

4.1. Vector Current Compare

We collected dataset at location A (the common coverage area of the two radar sites) from 2009-8-26 06:28:08 to 2009-8-28 08:00:00 (low tide) and from 2009-09-03 06:00:00 to 2009-09-05 08:00:00 (high tide).

The scatter diagram in Fig. 4(a) with 322 samples collected in 5 days shows the relationship between the current velocity estimated by radar and that recorded by ADCP. The correlation coefficient between the two is 0.86 with RMS differences less than 10 cm/s. The slope of

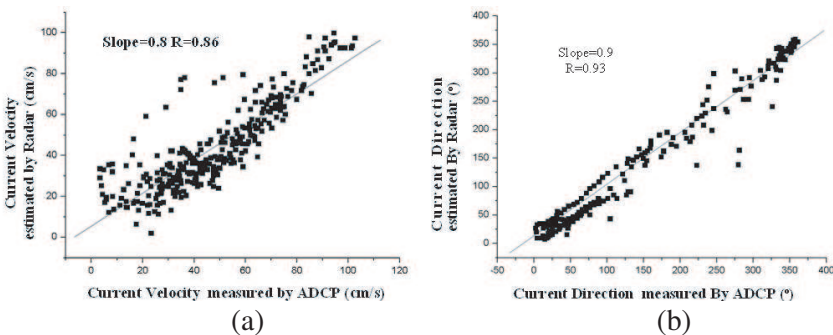


Figure 4. Scatter plot and linear regression of current parameters estimated by HF-Radar vs. parameters recorded by ADCP. R means correlation coefficient. (a) Current velocity. (b) Current direction.

the regression line in Fig. 4(a) is 0.8. The scatter diagram in Fig. 4(b) shows the relationship between the current direction estimated by radar and that recorded by ADCP. The correlation coefficient is 0.93 with RMS differences less than 12°. The slope of the regression line in Fig. 4(b) is 0.9. These results are in accord with recent results [7–9]. Fig. 4(a) shows that some obvious discrepancies occur when the current velocity is less than 10 cm/s or more than 90 cm/s, which may be due to the different sampling methods adopted by the two instruments, as HF radar data provides time average samples over ten minutes while ADCP provides instantaneous samples. Despite the possible errors, the statistical relationship of slope and correlation coefficient of the regression indicates that the HF radar captured the real current variation around location A.

4.2. The Mean Absolute Errors at Different Water Depths

In order to investigate what is the ‘effective depth’ below the surface that HF radar estimated, we compare surface currents estimated by HF radar and subsurface currents measured by different bins (from 1 m to 6 m in depth) of a bottom-mounted ADCP on point A in 20-m water depth. The mean absolute errors of current velocity and direction at different depths are shown in Figs. 5(a) and 5(b). Curves 1 to 6 in Fig. 5(a) show the impact of depth on current velocity distribution. Curve 1 means “radial current velocity, Shengshan Island, low tide”, which is the radial current velocity estimated by radar located at

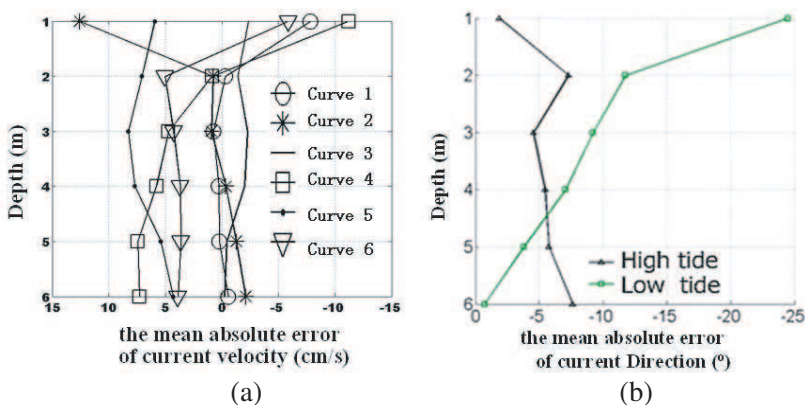


Figure 5. (a) The mean absolute error of current velocity vs depth; (b) the mean absolute error of current direction vs depth.

Shengshan Island during the low tide. Curve 2 means “radial current velocity, Zhujiajian Island, low tide”. Curve 3 means radial current velocity, Shengshan Island, high tide”. Curve 4 means radial current velocity, Zhujiajian Island, high tide”. Curve 5 means “vector current velocity, high tide”, and Curve 6 means “vector current velocity, low tide”. According to Fig. 5(a), the mean absolute errors of current velocity are smaller than 10 cm/s except those in depth of 1 m. In Fig. 5(b), curves labeled “low tide” and “high tide” show the impact of depth on mean absolute errors of current direction at different depths. The mean absolute errors of current directions during high tide and low tide are smaller than 12° for many depths except those in depth of 1 m. This can be explained in part by the influence of the surface wind or wave. Total results predict that the effective depth of current observed by TDMF radar is between 2 m and 6 m.

4.3. Comparing with Drifter

In order to track a subsurface current, a drifter was launched at point p1, and the total recorded data consisted of 12 hours of data from 2009-9-03 06:00:08 to 2009-9-03 19:00:00. A good agreement between radar and drifter data is shown in Fig. 6. As shown in Fig. 6(a), the current velocity started at 42 cm/s, increased to 58 cm/s, and then decreased back to 4 cm/s, and such a change continued, which shows that the vector current obtained with the OSMAR2009 radar can track the major features of the drifter measurements very well. About the current direction, according to Fig. 6(b), the drifter measure data and radar data (their correlation coefficient is 0.92) both increased from 0° to 360° , followed by another identical period, which indicates the continuous rotation of the current.

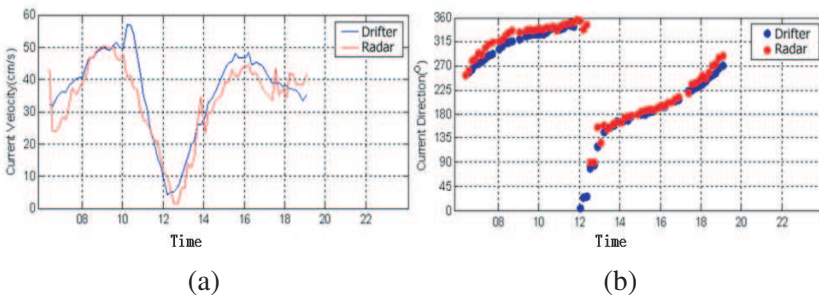


Figure 6. (a) Current velocity estimated by radar vs Current velocity recorded by drifter. (b) Current direction estimated by radar vs Current direction recorded by drifter.

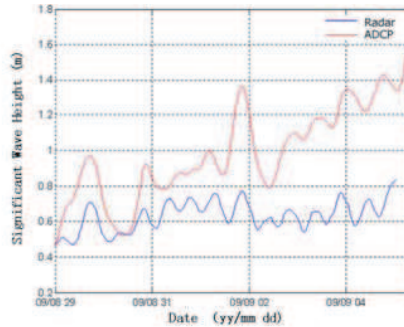


Figure 7. Compare of significant wave height estimated by radar and that recorded by ADCP.

4.4. Significant Wave Height Measuring

Wave height measurement requires better signal to noise (SNR) of the backscatter signal than current measurement and a more complex inversion process in which the inversion of Barrick's second-order equation is inevitable [10]. Howell method [11] views a spectral factor as a constant to linearize the Barrick's equation, yet it is only applicable to the radar of higher frequency. Green method [12], which discretizes the second order equation utilizing the image reconstruction technology, is employed in osmar2009. With the Green method, a large sparsely matrix equation is obtained to inverse the directional spectrum by the ART (Algebraic reconstruction technique) [13]. The significant wave height (SWH) is then estimated based on the directional spectrum.

The measured point is about 10 km far from the radar site located at Zhujiajian Island, and the sea floor is about 20 m in depth. The measure time was from 2009-8-29 00:00:00 to 2009-9-05 07:00:00, and the Significant Wave Height (SWH) was sampled every hour by ADCP. Fig. 7 shows the similarity of SWH change between radar estimated and ADCP recorded. But SWH estimated by the radar is obviously smaller than that recorded by ADCP, which indicates that the results need a calibration, and the exact reason requires further study.

5. SUMMARY AND CONCLUDING REMARKS

The TDMF radar system, which employs multiple frequencies, has been successfully installed and operated, and some preliminary results have been acquired in East China Sea. In this paper, a comparison is presented between TDMF radar data and instruments data, including

current velocity, current direction and SWH sampled at the same time and location. The statistics of current velocity computed over the whole data set are characterized by a RMS difference smaller than 12 cm/s and a correlation coefficient greater than 0.80. Compared to previous values reported in the literature (Recent studies show significant variability in the results, with RMS differences between radar and other platforms ranging between 5 and 20 cm/s [14–16]), the RMS values are in the same spectrum but definitely at the smaller end. The current direction value estimated by TDMF radar meets the demands of the ocean researchers.

To summarize, the results indicate that the data estimated by TDMF radar accord with the data recorded by traditional instruments and that they appear well suited for the study of coastal areas with complex patterns of velocity and transport.

However, differences between TDMF radar and other platforms are expected to occur for a number of reasons. First, all the platforms have measurement errors. Second, radars have limited radial velocity resolution (a few cm/s) due to frequency resolution, while instruments have slippage errors of few cm/s [17]. Third, HF radar provides time averages data over CITs of typical 10 minutes, while ADCPs or drifters provide instantaneous information. In addition, the SWH inversion also needs a calibration. Therefore, further research is needed to improve the detection ability of TDMF radar.

ACKNOWLEDGMENT

This project is supported by the 863 High Technology Project of China and by LIESMARS Special Research Funding. The TDMF radar is the outcome of many years of dedicated effort by my colleagues in Wuhan University. The authors are grateful for the support given by Prof. Z. J. Yang, Prof. H. Y. Ke and others. The authors would also like to thank the reviewers for many helpful comments and suggestions, which have enhanced the quality and readability of this paper.

REFERENCES

1. Liang, D., P. Xu, L. Tsang, Z. Gui, and K.-S. Chen, "Electromagnetic scattering by rough surfaces with large heights and slopes with applications to microwave remote sensing of rough surface over layered media," *Progress In Electromagnetics Research*, PIER 95, 199–218, 2009.
2. Wu, Z.-S., J.-J. Zhang, and L. Zhao, "Composite electromagnetic scattering from the plate target above a one-dimensional sea

- surface: Taking the diffraction into account,” *Progress In Electromagnetics Research*, PIER 92, 317–331, 2009.
3. Chen, H., M. Zhang, D. Nie, and H.-C. Yin, “Robust semi-deterministic facet model for fast estimation on EM scattering from ocean-like surface,” *Progress In Electromagnetics Research B*, Vol. 18, 347–363, 2009.
 4. Yang, S., H. Ke, X. Wu, J. Tian, and J. Hou, “HF radar ocean current algorithm based on MUSIC and the validation experiments,” *IEEE Journal of Oceanic Engineering*, Vol. 30, No. 3, 601–617, 2005.
 5. Teague, C. C., J. F. Vesecky, and Z. R. Hallock, “A comparison of multifrequency HF radar and ADCP measurements of near-surface currents during COPE-3,” *IEEE J. of Oceanic Eng.*, Vol. 26, No. 3, 399–405, July 2001.
 6. Zhang, X., G. Feng, and D. Xu, “Blind direction of angle and time delay estimation algorithm for uniform linear array employing multi-invariance MUSIC,” *Progress In Electromagnetics Research Letters*, Vol. 13, 11–20, 2010.
 7. Mau, J.-C., D.-P. Wang, D. S. Ullman, and D. L. Codiga, “Comparison of observed (HF radar, ADCP) and model barotropic tidal currents in the New York bight and block island sound,” *Estuarine, Coastal and Shelf Science*, Vol. 72, 129–137, 2007.
 8. Son, Y.-T., S.-H. Lee, C.-S. Kim, J. C. Lee, and G.-H. Lee, “Surface current variability in the Keum River Estuary (South Korea) during summer 2002 as observed by high-frequency radar and coastal monitoring buoy,” *Continental Shelf Research*, Vol. 27, 43–63, 2007.
 9. Mau, J.-C., D.-P. Wang, D. S. Ullman, et al., “Model of the long island sound outflow: Comparison with year-long HF radar and doppler current observation,” *Continental Shelf Research*, Vol. 28, 1791–1799, 2008.
 10. Barrick, D. E., “Dependence of second-order sidebands in HF sea echo upon sea state,” *IEEE G-AP Int. Symp. Digest.*, 194–197, 1971.
 11. Howell, R. and J. Walsh, “Measurement of ocean wave spectra using narrow-beam HF radar,” *IEEE J. Oceanic Eng.*, Vol. 18, 296–305, 1993.
 12. Green, J. J., “Discretising Barrick’s equations,” *Proceedings of Wind over Waves II: Forecasting and Fundamentals of Applications*, 219–232, S. G. Sajjadi and J. C. R. Hunt (eds.), IMA and Horwood, 2003.

13. Green, J. J. and L. R. Wyatt, "Row-action inversion of the Barrick-Weber equations," *American Meteorological Society*, March, 2006.
14. Essen, H. H., K. W. Gurgel, and T. Schlick, "On the accuracy of current measurements by means of HF radar," *IEEE J. Oceanic Eng.*, Vol. 25, 472–480, 2000.
15. Emery, B. M., L. Washburn, and J. A. Harlan, "Evaluating radial current measurements from CODAR high-frequency radars with moored current meters," *J. Atmos. Ocean. Technol.*, Vol. 21, 1259–1271, 2004.
16. Shay, L. K., J. Martinez-Pedraja, T. M. Cook, and B. K. Haus, "High-frequency radar mapping of surface currents using WERA," *J. Atmos. Ocean. Technol.*, Vol. 24, 484–503, 2007.
17. Poulain, P. M., R. Gerin, E. Mauri, and R. Pennel, "Wind effects on drogued and undrogued drifters in the eastern mediterranean," *J. Atmos. Oceanic Technol.*, Vol. 26, 1144–1156, 2009.